MECHANICAL BEHAVIOR MODELING OF UNIDIRECTIONAL CARBON FIBER REINFORCED POLYMER COMPOSITES REINFORCED WITH Z-DIRECTIONAL NANOFIBERS

Fariborz Bayat, Kuang-Ting Hsiao*
University of South Alabama
150 Jaguar Drive
Mobile, Alabama 36688, United States
*Corresponding Author: Email: kthsiao@southalabama.edu, Phone: 1-251-460-7889

ABSTRACT

This paper utilizes a periodic unit cell modeling technique combined with finite element analysis (FEA) to predict and understand the mechanical behaviors of a nanotechnology-enhanced carbon fiber reinforced polymers (CFRPs) composite. This research specifically focuses on the study of novel Z-threaded CFRPs (ZT-CFRPs) that are reinforced not only by unidirectional carbon fibers but also with numerous carbon nanofibers (CNFs) threading through the CFRP laminate in the z-direction (i.e., through-thickness direction). The complex multi-scaled orthogonally-structured carbon reinforced polymer composite is modeled starting from a periodic unit cell, which is the smallest periodic building-block representation of the material. The ZT-CFRP unit cell includes three major components, i.e., carbon fibers, polymer matrix, and carbon nanofiber Z-threads. To compare the mechanical behavior of ZT-CFRPs against unmodified, control CFRPs, an additional unit cell without CNF reinforcement was also created and analyzed. The unit cells were then meshed into finite element models and subjected to different loading conditions to predict the interaction among all their components. The elastic moduli of both unit-cells in the z-direction were calculated from the FEA data. By assuming the CNFs have the same mechanical properties of T-300 carbon fiber, the numerical modeling showed that the ZT-CFRPs exhibited a 14% improvement in z-directional elastic modulus due to the inclusion of 1 wt% CNF z-threads, indicating that ZT-CFRPs are stiffer compared to control CFRPs consisting of T-300 carbon fibers and epoxy.

1. INTRODUCTION

Carbon fiber reinforced polymers (CFRPs) possess high modulus-to-weight and strength-to-weight ratios, which have led to an increased rate of utilization of these materials in different industrial fields, such as the automotive and aerospace industries where weight-saving is crucial [1]. Although CFRPs possess desirable material properties in the direction of carbon fiber reinforcement (i.e., x-direction), they are strictly limited in the thickness direction (i.e., z-direction), which lacks the carbon fiber reinforcements. Utilizing carbon nanofiber (CNF) z-threads is a new reinforcement technique that has been shown to considerably improve certain mechanical and electrical properties of CFRPs [2,3]. CNF z-threaded CFRPs (ZT-CFRPs)

possess CNFs that are transversely oriented (i.e., the z-direction) through the thickness of the CFRP laminate. These CNFs are suggested to provide significant improvements to mechanical, electrical, and thermal properties of CFRP composites even at low CNF concentrations. Hsiao et al. [2] have shown that CFRPs containing 0.3 wt% CNF z-threads (measured as a percentage of matrix weight) exhibited a 29% improvement in Mode-I delamination toughness compared to unmodified control CFRPs and meanwhile reduced the coefficient of variation by 12%. In addition, Scruggs et al. [3] illustrated that CFRPs containing 0.1 wt % CNF z-threads exhibited a 238 % increase in through-thickness DC electrical conductivity compared to control CFRPs, while also reducing the coefficient of variation by 14 %. In all cases, it was found that a small amount of CNF z-threads not only improved the z-directional properties but also reduced the property uncertainty, which is caused by lacking z-directional fiber reinforcement in traditional CFRP laminates (i.e., control CFRPs).

The goal of this study is to analyze the mechanical behavior of ZT-CFRPs at the micromechanics level by using numerical modeling techniques and finite element analysis (FEA) through SolidWorks and ANSYS Workbench. Composite materials may be analyzed at the laminate, lamina or micro level; however, the complex geometrical arrangements existing among different constituents within ZT-CFRPs, requires that these materials first be analyzed at the microstructure level to better understand their behavior at the smallest scale.

To model the microstructure of ZT-CFRPs, a unit cell design was developed to accurately represent the geometric relationships among the carbon fibers, matrix and CNFs. On the other hand, to contrast the effects of adding CNF z-threads to a CFRP microstructure, another unit cell was designed to represent the microstructure of an unmodified, control CFRP. After assembling both unit cells, they were subjected to specific loading conditions; under which their FEA simulated responses were then compared. The following sections explain the utilized method in further detail.

2. MODELING TECHNIQUE

The unit cell approach is one of the most popular methods in modeling the microstructures of composite materials. The behaviors of these materials have been analyzed in numerous studies using different unit cell approaches. For instance, Jayendiran and Arockiarajan [4] studied the viscoelastic behavior of piezocomposites by utilizing a unit cell model containing a single cylindrical piezoelectric rod enclosed by a polymer matrix, while Vivo et al. [5] analyzed the electrical properties of carbon nanotube-filled composites with a 3D cubical cell consisting of a matrix material that was embedded with several small randomly distributed cylindrical nanotubes. Similarly, R. Simoes et al. [6] studied the electrical behavior of an amorphous polymer containing linear rod volumes, which represented the carbon nanofibers, using a 3D unit cell model. Other unit cell approach examples cover topics such as electromagnetic behavior of carbon fiber reinforced plastics, where unit cells with interlacing and non-interlacing carbon fiber weaves were modeled and analyzed [7], and the nanoindentation behaviors of single wall carbon nanotubes [8], which were studied with a 3D unit cell containing a polymer matrix, a single-wall carbon nanotube inclusion, and an interphase connecting the two.

The discussed studies utilized different unit cell approaches for a wide variety of applications, however they utilized simple geometries, such as straight cylindrical nanofibers, in their unit cell

models which cannot be used to accurately model the CFRPs under investigation in this study. The ZT-CFRPs invested in this study, with above 60% carbon fiber volume fraction and relatively packed carbon fibers, possess complex multiscale structural geometries that require a unique unit cell design to appropriately represent the microstructure. Material properties and the geometry of the real microstructure of ZT-CFRPs were to be studied as the initial step in the design process of the unit cell assembly. These CFRPs are constructed from the T300 carbon fiber, Epon 862/epicure-W epoxy resin, and PR-24-XT-PS CNFs. The material properties of different constituent materials used to create the unit cells have been presented in Table 1. Note that no literature sources have quantified the properties of the PR-24-XT-PS CNFs. For this reason, the CNFs have been assumed with the properties of the T-300 carbon fibers in this modeling study. However, one should keep in mind that carbon nanofibers and carbon nanotubes could theoretically possess better physical properties than T-300 carbon fibers and the results form this study could be relatively conservative due to the assumption of CNF's mechanical properties based on T-300 carbon fiber.

Table 1. The material properties used to create the components within the modeled composite.

Material	Modulus of Elasticity (GPa)	Poisson's Ratio	Density (kg/m^3)	Sources
Carbon Fiber (T-300)	231	0.2	1760	[9]
CNF	Assumed to be the same as T-300 carbon fiber's properties			
Matrix (Cast Epoxy)	3.425	0.32	1250	[10]

To accurately design the unit cells, microscopic images served as the initial tools to help understand the geometrical arrangement within the material. Fig 1 represents one such image obtained in the lab and shows the arrangement of the T300 fibers inside the epoxy resin.

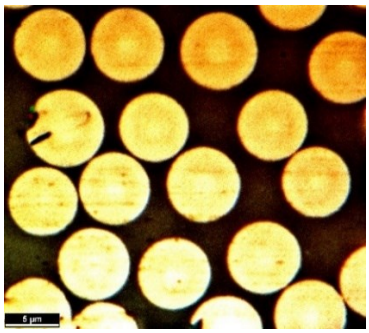

Fig. 1. Micrograph of the geometric arrangement of T300 fibers inside Epon 862 resin.

From these images, a unit cell made of five carbon fibers surrounded by matrix was initially constructed as shown in Fig. 2a. Despite the unit cell's decent representation of the composite microstructure, it was not suitable for modeling purposes since it was not periodic and could not be combined with other cells to form the composite lamina. For this reason, the correct periodic unit cell was constructed by cutting the indicated square piece out of the initial model as shown in Fig. 2b. The new cell contained one whole central fiber and four quarter-fibers in each corner and could easily be added to like cells to build the composite lamina as presented in Fig. 3.

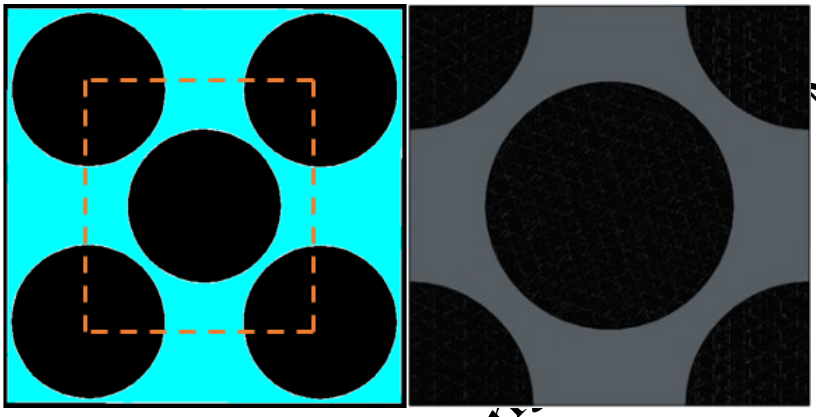

Fig. 2. (a) The original unit cell with an orange square indicating the region from which the periodic unit cell was constructed **(b)** The periodic unit cell

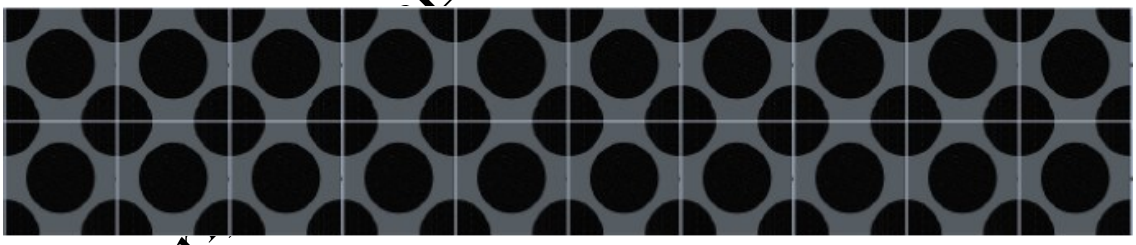

Fig. 3. A composite lamina formed by several periodic unit cells

While the geometry of the unit cell was designed at this stage, the dimensional relations among its different components were still undetermined. This problem was tackled by selecting a carbon fiber volume fraction of 60 %, which is very commonly used in CFRPs. Using the volume fraction relationship shown in Eq. 1, the matrix volume fraction was determined to be 40 %. Note that V_f and V_m refer to the fiber and matrix volume fractions, respectively.

$$V_f + V_m = 1 \quad [1]$$

The established shape of the periodic unit cell and the obtained volume percentage values led to two full cylindrical fiber volumes occupying 60 % of the unit cell volume. This relationship is presented in Eq. 2 where a represents the length of the sides of the unit cell and d_f represents the diameter of the carbon fiber.

$$2\left(\frac{(\pi d_f^2)}{4}a\right) = V_f(a^3) \quad [2]$$

Solving Eq. 2 for a yields Eq. 3, which establishes a relationship between the sides of the unit cell and the diameter of the carbon fiber.

$$a = d_f\sqrt{\frac{\pi}{2V_f}} \quad [3]$$

The volume fraction of the CNFs was assumed to be 0.5 % of the total matrix volume, which will give the weight fraction close to 1 wt% [2] w.r.t. the matrix. The above observations resulted in acquiring equations 4, 5, and 6 which helped in calculating the total volume of carbon nanofibers, V_n, the volume of a single carbon nanofiber, $V_{single\ nanofiber}$, and the number of carbon nanofibers needed inside the unit cell, respectively.

$$\mathrm{V}_n = 0.005\mathrm{V}_m \quad [4]$$

$$\mathrm{V}_{single\ nanofiber} = \left(\frac{\pi d_n^2}{4}\right)a \quad [5]$$

$$Number\ of\ Nanofibers = \frac{\mathrm{V}_n}{\mathrm{V}_{single\ nanofiber}} \quad [6]$$

Important dimensions of the components of the unit cell along with their calculated quantities are presented in Tables 2 and 3. Note that the dimensions were later scaled up to the mm level due to modeling limitations of the software used.

Table 2. Dimensions of the different components of the unit cell.

Parameters	Symbol	Value	Units
Fiber Diameter	d_f	7	μm
Unit Cell Sides Length	a	11.326	μm
Nanofiber Diameter	d_n	0.1	μm

Table 3. The quantity of each constituting component of the unit cell.

Components of the unit cell	Quantity
Matrix	1
Fiber	2 (1 whole and 4 quarter cylinders)
Nanofiber	32

The initial unit cell containing the matrix and fibers was constructed based on the above presented dimensions and quantities and is shown in Figure 4. Note that this unit cell represents an unmodified, control CFRP.

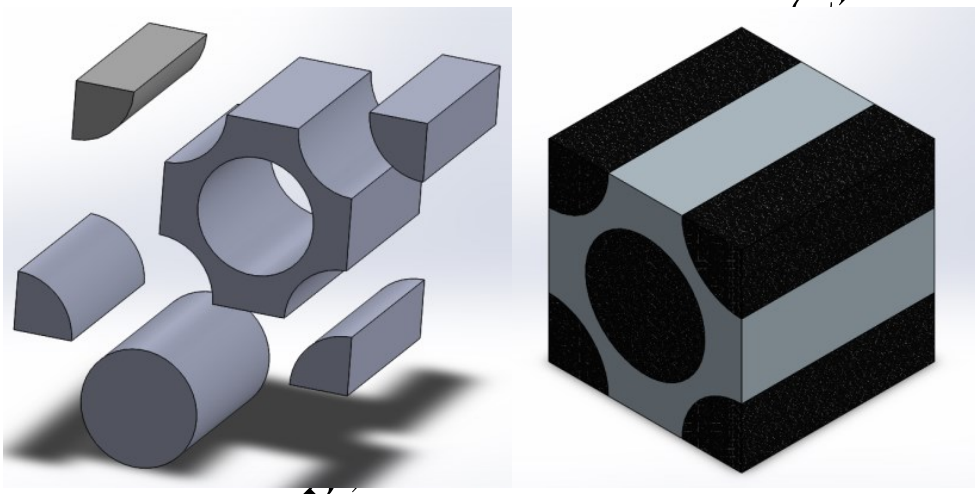

Fig. 4. Carbon fibers (1 full and 4 quarter cylinders) shown in black and matrix shown in gray within the control CFRP unit cell assembly

Although, at this point the base unit cell was assembled, the CNFs were yet to be designed and placed inside the cell to create the real microstructure representation of the ZT-CFRPs. Similar to the procedure utilized to investigate the fiber-matrix dimensional relationships, the development of the complex CNF parts was also to be in close agreement with the real shape of these entities. ZT-CFRPs are created by flow transferring a sheet of B-stage resin containing electric field aligned CNFs through a highly packed carbon fiber bed in the thickness direction [2]. Due to the limited space available among the carbon fibers within these fiber beds, the CNFs do not have a straight line of travel through the fiber bed. Thus, the CNFs must go through the channels among carbon fibers in a zig-zag way during the flow transfer process while still maintaining their overall z-direction orientation. This creates a zig-zag z-threaded microstructure as illustrated in Fig. 5.

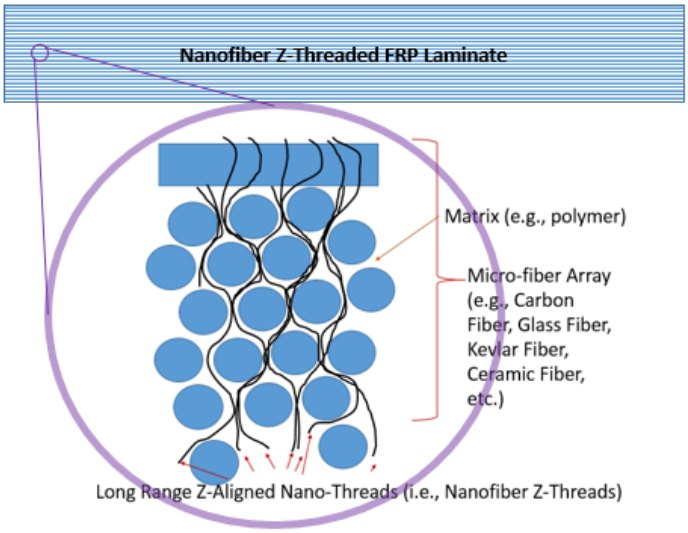

Fig. 5. Generalized schematic of the z-threaded CNF microstructure present within ZT-CFRPs.

Knowing the arrangement of CNF z-threads within the microstructure of the ZT-CFRPs, it becomes clear that one cannot simply use the common modeling approach and utilize straight cylindrical volumes to represent them. Accordingly, the CNFs were designed to embody the zig-zag threaded orientation shown in Fig. 5. The symmetric geometry of the designed CNF, accompanied by the lengths and radiuses of curvatures of its different portions, is shown in Fig. 6. At this stage, with the CNF geometries created, the final periodic unit cell could be constructed.

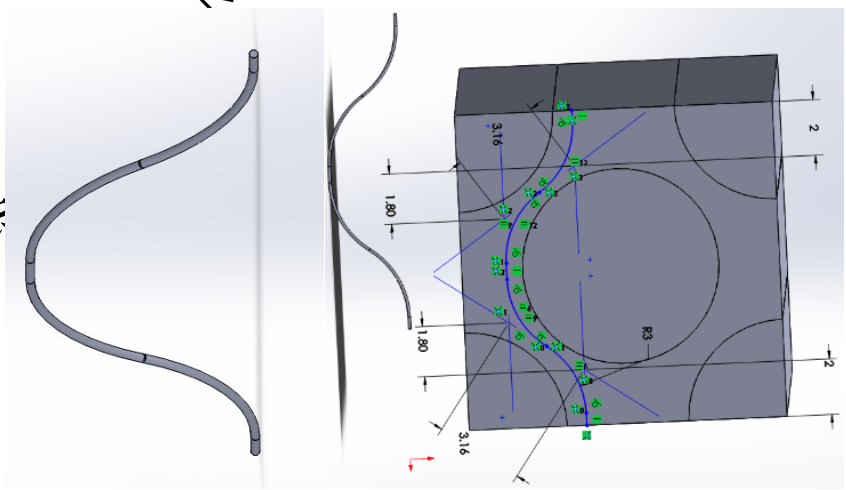

Fig. 6. The designed carbon nanofiber is presented, along with the dimensions (mm) of its different sections.

3. UNIT CELL ASSEMBLY

The final unit cell assembly representing the microstructure of the ZT-CFRP was created by embedding 32 CNFs throughout the matrix at a distance 0.67 mm apart from each other and 0.60 mm apart from the carbon fibers located in the corners of the unit cell as shown in Figure 7a.

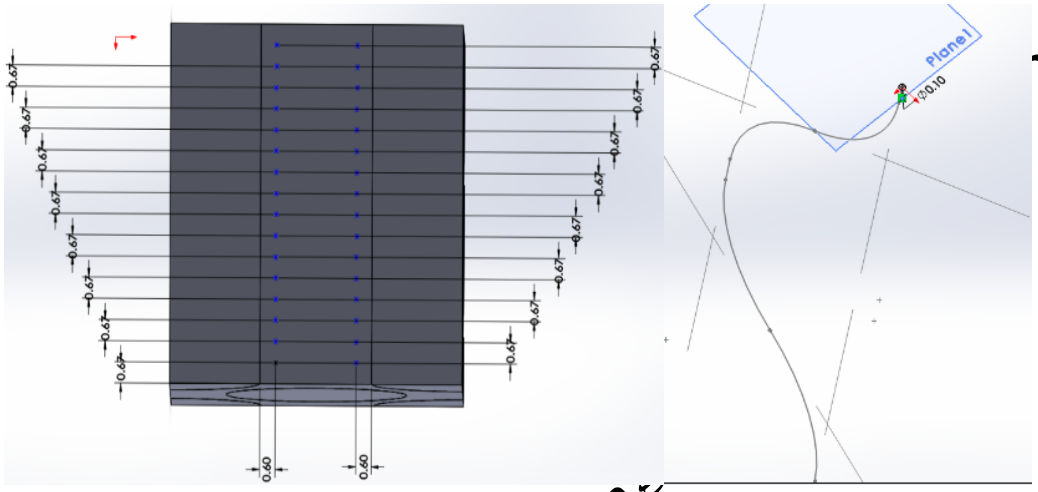

Fig. 7. (a) Top view of the unit cell presenting the set locations for CNF placements (b) The creation of the void volumes inside the unit cell using the sweep cut function.

The planned spaces matching the exact shapes of the nanofibers needed to first be cut out of the unit cell to allow the placements of the nanofibers inside the matrix. This was accomplished through the utilization of the sweep cut function within SolidWorks by defining both the circular cross sections of the CNFs (having a radius of 0.1 mm) and a path to follow their shape along their longitudinal axis. Two planes were defined, one defining the cross-sectional area of the CNF and the other defining its placement location and the path through which it would go through the thickness of the cell as shown in Figure 7b. The complex shapes of the CNFs and the precision needed to place them at their anticipated locations demanded this process to be repeated for each CNF z-thread, resulting in a total of 32 sweep cut operations.

Next, the CNF volumes were placed inside the cell using the mate function, which helped in bonding the CNF volumes to the matrix such that they were firmly secured in their new locations. Numerous coincident mates were used to place different planar surfaces of the two components (CNFs and the unit cell assembly) on the same plane, making them coplanar. Finally, combining the 32 newly added CNFs with the existing matrix and fiber components resulted in the creation of the ZT-CFRP unit cell presented in Fig. 8.

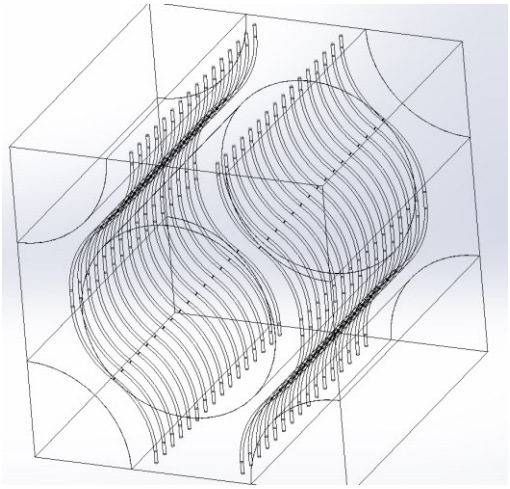

Fig. 8. The ZT-CFRP unit cell assembly containing 32 carbon nanofiber components

At this point, the material properties presented in Table 2 were assigned to the corresponding components and the unit cell was meshed using a refined curvature mesh, as shown in Fig. 9.

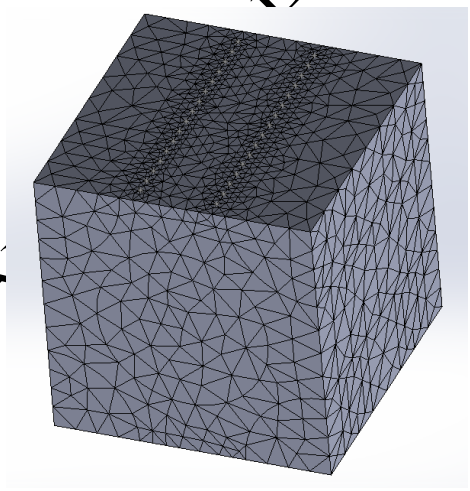

Fig. 9. A refined curvature mesh was utilized to mesh the structure of the unit cell.

Before performing the final FEA analysis, the integrity of the composite microstructure had to be confirmed. For this reason, a mesh convergence test was performed to ensure that the unit cell model had been well put together and that the boundaries among different unit cell components were well defined and did not result in any major error. This was accomplished by applying the

properties of the matrix material to all FEA elements (including carbon fibers, nanofibers, and the matrix) in both the control CFRP unit cell and the ZT-CFRP unit cell. A 1 % tensile displacement load was then applied to the top surface of both unit cells leading to the FEA results presented in Table 4.

Table 4. The results of the mesh convergence test comparing the average properties obtained for both control CFRP and ZT-CFRP unit cells.

Property	Control CFRP unit cell*	ZT-CFRP unit cell*
Equivalent Stress (MPa)	34.2	34.2
Normal Stress (MPa)	34.2	34.2
Equivalent Strain	9.99E-03	9.98E-03
Normal Strain	9.99E-03	9.97E-03

*For this mesh convergence FEA test, the matrix's properties are applied to all FEA elements

The obtained results were sufficiently close, indicating an error of less than 0.2 % sustained among the average stress and strain values experienced by both unit cells. This confirmed that the boundary areas between the matrix and CNFs, were well defined and therefore did not result in any significant error. The performed test approved that both control CFRP unit cell and the ZT-CFRP unit cell FEA models were created properly and were ready for further numerical simulations on the composites' mechanical behaviors.

4. RESULTS

Utilizing the ANSYS Workbench, the FEA was implemented starting with a series of boundary conditions, which were applied to the bottom surface of the unit cell to secure it in place while allowing its free deformation in all directions. The analysis was initially performed on a single unit cell and by applying a 1 % tensile displacement load to its top surface. However, a real microstructure of the composite would not be isolated while undergoing different loading conditions, as there would be other surrounding unit cells interacting with it to create symmetrical boundary conditions. Disregarding this symmetrical boundary requirement could result in sources of error during analysis, such as inaccurate, nonsymmetrical deformations along the sides of the unit cell under investigation. Hence, four additional unit cells were created and attached to the targeted cell to prevent the risk of such non-symmetrical errors and further improve the analysis as presented in Figure 10. A similar procedure as the one discussed for the single cell scenario was performed for applying boundary conditions and loads to the five-unit cell assembly. Fig. 10a and Fig. 10b illustrate the FEA schematics of the deformations of the five-unit cell assembly and the central unit cell respectively. Note that due to the load acting on the top surfaces, the top portions of the cells experienced maximum displacement as indicated by the red color

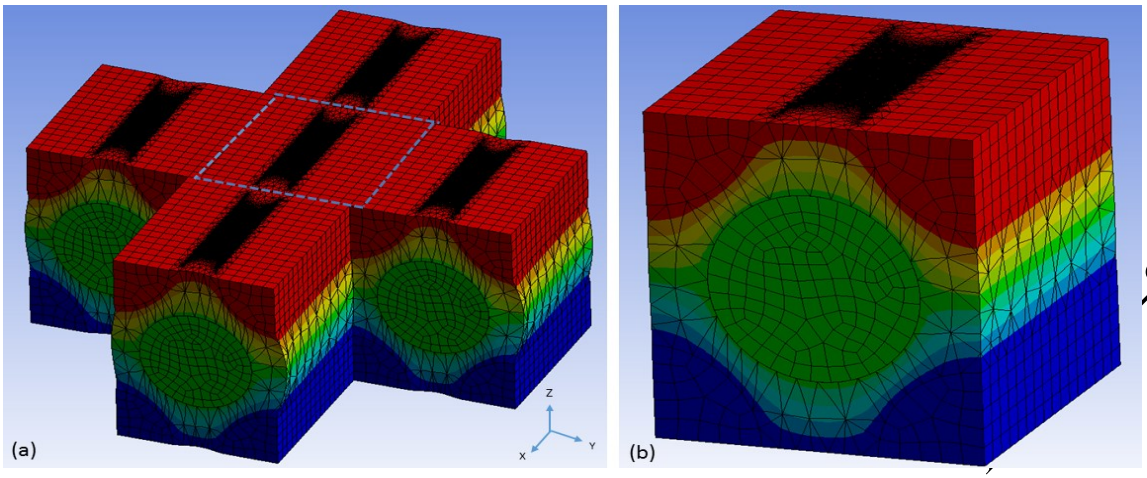

Fig. 10. (a) Deformation of all five-unit cells in the Z-direction. **(b)** The deformation of the targeted central unit cell

It can be observed from the above figure that due to the interactions of the neighboring cells, the central cell has experienced uniform deformation on all sides; however, this is not the case for the surrounding cells, as nonsymmetrical regions are observed on their outer faces. This observation highlights the importance of the five-unit cell assembly approach utilized in this modeling. The new approach was similarly implemented for both the control CFRP and the ZT-CFRP to investigate the improvements resulting from the presence of the CNF z-threads.

The most essential property needed to analyze and compare the mechanical characteristics of the two types of CFRPs was the modulus of elasticity. To obtain this property of the targeted unit cell, first the average stress values experienced by both unit cell types were evaluated using the relationship provided by Mallick [10].

$$\sigma_{avg} = \sigma_m \frac{A_m}{A_{total}} + \sigma_{cf} \frac{A_{cf}}{A_{total}} + \sigma_{cnf} \frac{A_{cnf}}{A_{total}} \quad [7]$$

Within Eq. 7, σ_m, σ_{cf} and σ_{cnf} represent the average normal stress values in the z-direction experienced by the matrix, carbon fiber and carbon nanofiber portions of the top surface, while σ_{avg} is the average stress experienced by the entire top surface of the unit cell. Similarly, A_m, A_{cf} and A_{cnf} represent the corresponding matrix, carbon fiber and carbon nanofiber areas of the top surface while A_{total} is the total area of the top surface of the unit cell. The calculated average z-directional normal stress values experienced by both unit cell types were then divided by the 0.01 strain value (resulting from the 1 % displacement load) to compute the z-directional moduli of elasticity values, which are shown in Table 5.

Table 5. Data utilized to calculate the z-directional modulus of elasticity of both unit cell types.

Unit Cells	Components	Stress, σ_{zz} (Pa)	Area, A (m^2)	Average Stress, $\sigma_{avg,zz}$ (Pa)	Modulus of Elasticity, E_{zz} (Pa)*	Modulus of Elasticity Improvement
Control CFRP	Matrix	6.44E+7	4.9E-5	1.04E+8	1.04E+10	14.2 %
	Carbon Fiber	1.29E+8	7.93E-5			
ZT-CFRP	Matrix	7.89E+7	4.87E-5	1.19E+8	1.19E+10	
	Carbon Fiber	1.33E+8	7.93E-5			
	CNF	3.51E+9	2.51E-7			

*Strain value of 0.01 experienced by both unit cells was utilized to calculate the modulus of elasticity

The results indicate an improvement of more than 14% in the z-directional modulus of elasticity of the ZT-CFRP due to the addition of the 0.5 vol% CNF z-threads. Note that the 0.5 vol% is w.r.t. the total matrix volume, which is 40 vol% of the total composite volume. Therefore, the CNF z-threads has a very low volume fraction of 0.2 vol% w.r.t. the total composite volume in this modeling study. The results clearly indicated that CNF z-threads, even with a low volume fraction, have a substantially positive effect on the mechanical properties of CFRPs.

5. CONCLUSIONS

Through FEA, this study investigated the effects of CNF z-threads on the mechanical behavior of CFRPs. This was accomplished by evaluating and comparing the z-directional moduli of elasticity of both newly developed CNF z-threaded CFRPs (ZT-CFRPs) and unmodified, control CFRPs. Through examination of the composite structure at the microscopic level, the unit cell approach was utilized to create and analyze the microstructure of the material. Two different types of unit cells were designed: (1) a control CFRP unit cell containing one plus four quarter cylindrical carbon fibers surrounded by an epoxy matrix material (for achieving 60% carbon fiber volume fraction) and (2) a ZT-CFRP containing 32 curved CNF z-threads added to the control CFRP unit cell (to achieve 0.5% CNF volume fraction w.r.t. the epoxy matrix, which is equivalent to 0.2 vol% w.r.t. the composite). A 1% tensile displacement load was applied to the top surfaces of each unit cell and the FEA results indicated that the ZT-CFRP exhibited a 14.2% increase in the z-directional modulus of elasticity over the control CFRP which was concluded to be solely due to the inclusion of the very small amount of CNF z-threads.

For the future work of this study, the unit cell modeling method introduced herein will be further used to evaluate additional mechanical properties of the ZT-CFRP composites, such as the values of Poisson's ratios and the moduli in other directions. A parametric study will also be conducted to investigate the composite's sensitivity in terms of property change while changing the material properties of one its components, such as the matrix. In addition, the mechanics of the composite material at the macrostructure will be investigated. Using the set of properties obtained at the microstructure level as the input data, the lamination theory will be utilized to evaluate the mechanical behavior of the ZT-CFRP lamina and laminate.

6. ACKNOWLEDGEMENT

The authors would like to thank the financial supports from Alabama Higher Education (Alabama GRSP program, Award number: 160336) and Alabama Department of Commerce (Alabama Innovation Fund, Award number: 150436).

7. REFERENCES

1. Bullen GN. "Advanced Materials for Aerospace and Space Applications." *SAE International Journal of Aerospace*, 2014.

2. Hsiao KT, Scruggs AM, Brewer JS, Hickman GJ, McDonald EE, Henderson K. "Effect of carbon nanofiber z-threads on mode-I delamination toughness of carbon fiber reinforced plastic laminates." *Composites Part A: Applied Science and Manufacturing* 2016.

3. Scruggs AM, Henderson K, Hsiao K-T. "Characterization of electrical conductivity of a carbon fiber reinforced plastic laminate reinforced with z-aligned carbon nanofibers." *Proceedings of CAMX 2016 (The Composites and Advanced Materials Expo).* Anaheim, CA, Sept. 26-29, 2016.

4. Jayendiran R, Arockiarajan A. "Viscoelastic modeling and experimental characterization of thermo-electromechanical response of 1–3 piezocomposites." *Journal of Applied Physics* 2014.

5. De Vivo B, Lamberti P, Spinelli G, Tucci V. "Numerical investigation on the influence factors of the electrical properties of carbon nanotubes-filled composites." *Journal of Applied Physics* 2013.

6. Simoes R, Silva J, Cadilhe A, Vaia R. "Applications of the graph theory to the prediction of electrical and dielectric properties of nano-filled polymers." *Composite Interfaces* 2010.

7. Hassan AM, Douglas JF, Garboczi EJ. "Computational modeling of the electromagnetic characteristics of carbon fiber-reinforced polymer composites with different weave structures." *AIP Conference Proceedings.* 2014.

8. Le MT, Huang SC. "Numerical Simulation of Nanoindentation of Single Wall Carbon Nanotube Reinforced Epoxy Composite." *Applied Mechanics and Materials* 2015.

9. Toray® T300 Data Sheet. Document CFA-001, 10 Nov. 2017.

10. Mallick PK. *Fiber-reinforced composites: materials, manufacturing, and design*. 3rd ed. CRC Press 2007.